Superlubric-Pinned Transition in Sliding Incommensurate Colloidal Monolayers

Davide Mandelli[1], Andrea Vanossi[2,1], Michele Invernizzi[3], S. V. Paronuzzi Ticco[1], Nicola Manini[3,1,2], Erio Tosatti[1,2,4]

[1] *International School for Advanced Studies (SISSA), Via Bonomea 265, 34136 Trieste, Italy*
[2] *CNR-IOM Democritos National Simulation Center, Via Bonomea 265, 34136 Trieste, Italy*
[3] *Dipartimento di Fisica, Università degli Studi di Milano, Via Celoria 16, 20133 Milano, Italy*
[4] *International Centre for Theoretical Physics (ICTP), Strada Costiera 11, 34014 Trieste, Italy*
(Dated: August 4, 2015)

Two-dimensional (2D) crystalline colloidal monolayers sliding over a laser-induced optical lattice providing the periodic "corrugation" potential recently emerged as a new tool for the study of friction between ideal crystal surfaces. Here we focus in particular on static friction, the minimal sliding force necessary to depin one lattice from the other. If the colloid and the optical lattices are mutually commensurate, the colloid sliding is always pinned by static friction; but when they are incommensurate the presence or absence of pinning can be expected to depend upon the system parameters, like in one-dimensional (1D) systems. If a 2D analogy to the mathematically established Aubry transition of one-dimensional systems were to hold, an increasing periodic corrugation strength U_0 should turn an initially free-sliding, superlubric colloid into a pinned state, where the static friction force goes from zero to finite through a well-defined dynamical phase transition. We address this problem by the simulated sliding of a realistic model 2D colloidal lattice, confirming the existence of a clear and sharp superlubric-pinned transition for increasing corrugation strength. Unlike the 1D Aubry transition which is continuous, the 2D transition exhibits a definite first-order character, with a jump of static friction. With no change of symmetry, the transition entails a structural character, with a sudden increase of the colloid-colloid interaction energy, accompanied by a compensating downward jump of the colloid-corrugation energy. The transition value for the corrugation amplitude U_0 depends upon the misalignment angle θ between the optical and the colloidal lattices, superlubricity surviving until larger corrugations for angles away from the energetically favored orientation, which is itself generally slightly misaligned, as shown in recent work. The observability of the superlubric-pinned colloid transition is proposed and discussed.

Keywords: 68.35.Af,68.60.Bs,64.70.Nd,83.85.Vb,82.70.Dd

I. INTRODUCTION

The great progress of nanofriction of the last decades has enabled increasing insight into the microscopic nature of friction.[1–3] In particular, the sliding between contacting crystalline surfaces has become of higher interest after the manipulation of nanoscale-sized objects revealed how the atomistic features of an interface may play the ultimate role in determining its tribological properties. Fresh interest is now generated by artificial but highly instructive systems represented by 2D colloidal monolayers sliding in an optical lattice, the main system which we use as a working example in this study.[4] Two atomically flat and perfect crystal surfaces in contact are commensurate when the mismatch ratio ρ between their lattice parameters is rational. Perfect matching ($\rho = 1$) between two lattices of same symmetry represents the simplest situation, where the atoms of one crystal lattice (the slider) perfectly fit the minima of the two-dimensional "corrugation" periodic potential landscape generated by the other lattice (see Fig. 1a). In this case a finite and large external force is required to dislodge the slider atoms from the potential minima, so as to nucleate, at finite temperature,[5,6] the onset of sliding.

A different situation arises when the periodicities of the two contacting lattices are mismatched, as is realized either by a value $\rho \neq 1$, or else by a mutual rotation of two lattices, as shown schematically in Fig. 1b. The
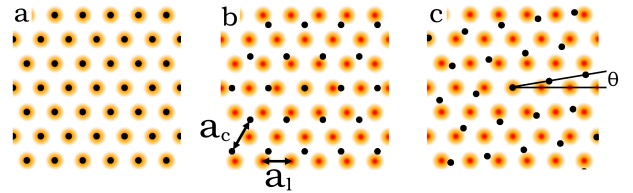

FIG. 1. (Color online) (a) Schematics of a $\rho = 1$ commensurate interface between a colloidal monolayer (black dots) and a triangular optical lattice potential (light spots correspond to the minima). (b) A colloidal monolayer of lattice spacing a_c with a mismatched triangular potential of periodicity $a_l = \rho a_c$. The two lattices are mismatched but aligned. (c) Colloidal monolayer with a small misfit angle θ with respect to the mismatched substrate. This kind of rotation generally lowers the energy and is a likely equilibrium feature.[18]

present study concerns interfaces that are incommensurate. A situation far more common in nature, it also naturally exhibits more interesting tribological features than commensurate ones.[7] We focus especially on static friction, the minimal sliding force necessary to depin one lattice from the other. The main issue we address here is the nature of static friction against sliding of a 2D lattice onto a 2D incommensurate corrugation.

The reference point for our understanding is the 1D case, epitomized by the so-called Frenkel-Kontorova (FK)

model, consisting of a harmonic chain of classical point particles in a static sinusoidal potential, an idealized system whose physics has been very widely studied and understood.[8] In 1D, the incommensurability between interparticle spacing and sinusoidal potential wavelength gives rise to a potential-induced deformation of the chain particle position, that can be described by a deformation of the chain's phase $\Phi(x)$ relative to that of the potential, from the non-interacting straight line of slope $(\rho-1)$ to a staircase with the same mean slope but formed by nearly horizontal, approximately constant phase terraces. These commensurate domains are separated by steps in the relative phase, often called solitons (or kinks) and antisolitons (or antikinks), where most of the misfit stress is concentrated.

This 1D system is known to display a remarkable dynamical phase transition, first described by Aubry.[9] When the corrugation is weak, below a critical magnitude, when the soliton widths are comparable to or larger than that of terraces and the overall phase modulation is small, the FK chain exhibits no pinning, the static friction is zero. In this regime one finds particles at all potential values, and all possible phases of the chain particles are accessible in dynamics. Since the total potential energy is independent of the phase, $\delta E/\delta\Phi = 0$, the chain as a whole can be displaced by any infinitesimal force. This absence of static friction has been dubbed "superlubricity".[10] However, above a critical corrugation magnitude, whose value depends on precise parameters and incommensurability, the chain develops a nonzero static friction through a continuous "Aubry" phase transition. The essence of the Aubry transition is that the probability to find a particle exactly at a potential maximum drops mathematically to zero (of course at $T=0$). Thus, even if $\delta E/\delta\Phi$ is still zero, this new dynamical constraint limits phase-space accessibility, breaking ergodicity in a way similar to a glass transition, with the onset of static friction and of chain pinning against free sliding. This transition is of a dynamical nature, so that even if the step-terrace deformation of the chain's phase $\Phi(x)$ becomes more marked in the pinned state, it still remains similar in nature to the superlubric one. Although suggestive, the static structure difference between the two does not reveal the essence of the transition. A more relevant signature is provided by the sliding friction. In the superlubric state, sliding of the chain occurs under any applied force however small, and can be envisaged as a state of flow of the solitons. Soliton motion causes dissipation, increasing with speed in correspondence with increasing emission of phonons. In the pinned state, chain sliding occurs only once the static friction force is overcome, at which point the sliding dynamics becomes generally quite different from the superlubric state.

In view of this well-known 1D case, it is physically clear that a qualitatively similar state of affairs should also occur in 2D incommensurate sliders. That is actually a case much more relevant in practice, where one expects free, superlubric sliding for weak corrugation, and

pinning with stick-slip for strong corrugation. Superlubricity is documented in several real 2D systems. Very small values of the static friction force F_s were observed for a rotationally misaligned graphene flake sliding over graphite,[11] the pinned configuration corresponding to the aligned and therefore commensurate case. Superlubricity and consequent ultra-low dynamic friction has also been demonstrated or implied in a number of cases, such as also telescopic sliding among carbon nanotubes,[12,13] in cluster nanomanipulation studies,[14,15] and in the sliding of rare-gas adsorbates.[16,17] However, there is no experimental case so far exhibiting a clear superlubric-pinned transition among 2D incommensurate sliders under fixed geometrical conditions. An experimental system of fresh relevance where that goal might be pursued is represented precisely by two-dimensional crystalline colloidal monolayers sliding over a laser-induced periodic corrugation potential. Measurements[4] and computer simulations[7] of colloidal monolayers interacting with a laser-induced periodic potential demonstrated the possibility to attain negligible values of the static friction force in incommensurate geometries. Therefore a study of the transition from the superlubric to the pinned state, done at constant lattice mismatch, and at constant mutual alignment is potentially feasible for sliding colloid monolayers. These systems are excellent candidates as they allow to change all the relevant parameters of the interface: the corrugation strength U_0 and the colloidal crystal lattice parameter a_c, which sets the mismatch ratio $\rho = a_l/a_c$ given the optical potential periodicity a_l, fixed by the laser. The mutual alignment or misalignment between the colloid and the optical lattices is decided by energetics. As was established by a recent study, a small misalignment generally prevails, directly detectable by the colloid moiré pattern.[18] This kind of misalignment, depicted in Fig. 1c, is well established in surface-adsorbed rare-gas monolayers.[19–21]

The question we address here, only marginally touched upon so far[8] is whether at constant mismatch the weak- and the strong-corrugation regimes will again or will not be separated by a well-defined superlubric–pinned phase transition of the same type as that described by Aubry in 1D – the only case where a mathematical treatment has been worked out. Colloid monolayers offers the ideal chance to verify this point if not analytically at least numerically in a realistic and relevant case.

For a 2D triangular crystal monolayer interacting with a mismatched rigid corrugation periodic potential the 1D soliton-terrace staircase is replaced by a 2D superlattice of nearly commensurate domains. The domains are separated by soliton (antisoliton) misfit dislocation lines, depending on the specific value of ρ, and of the misalignment angle. In triangular symmetry, three families of soliton lines, oriented at ± 120 degrees from one another, will generally coexist. The coincidence plot between the two lattices (monolayer and periodic corrugation) realizes a moiré pattern, consisting of a patchwork of nearly commensurate, roughly hexagonal domains separated by

the soliton lines, which concentrate the mismatch of the two lattices.[22] Like in 1D, the sliding of the 2D monolayer enacts a "flow" of the solitons in the moiré pattern. A spontaneous angular misalignment, which when present lowers the energy by increasing the interdigitation of the two lattices, strongly modifies that pattern and correspondingly increases friction.[18]

The main questions which we plan to address here are: (a) Is there a sharp superlubric-pinned transition in the sliding of incommensurate colloid monolayers for increasing corrugation strength? (b) Is this 2D transition continuous and critical (as in 1D), or first order? (c) Does the spontaneous misalignment affect the transition, and when so, to what effect?

Here we present simulations for a model incommensurate monolayer which show that: (a) Superlubricity is replaced by pinning through a sharp transition. (b) That transition is, at least for the set of parameters used, of first order rather than continuous. (c) Spontaneous rotations very definitely affect the transition point, decreasing its critical value of corrugation U_0.

The paper is organized as follows. In Sect. II we introduce the model and the protocols adopted in the molecular dynamics simulations. In Sect. III we present results which indicate a first-order structural transition taking place in the colloid monolayer as a function of increasing corrugation. Section IV discusses the coincidence between this structural transition and the first-order onset of a static friction force F_s. In Sect. V we describe the dependence of the static properties of the monolayer on the misalignment angle. Section VI contains a discussion of possible experimental verifications, as well as our final remarks and conclusions.

II. MODEL AND SIMULATIONS

We describe the colloidal dynamics using the same model and parameters as in Refs. 7 and 18. In short, the 2D layer of colloidal particles is represented by screened-Coulomb repulsive, classical point-like particles, moving in 2D in a periodic potential (the corrugation) of amplitude U_0, periodicity a_l, and triangular symmetry. The overdamped dynamics of these particles is generated by integrating $T = 0$ damped equations of motion, with a large viscous damping coefficient $\eta = 28$. All results are expressed in terms of the system of units defined in Table I of Ref. 18. Simulations were performed adopting 2D periodic boundary conditions (PBC). Any desired misalignment angle between the corrugation and the colloidal lattice is implemented by means of a suitably chosen supercell, built using a standard procedure as follows.[23] The two lattices are defined by the pairs of primitive vectors $\mathbf{a}_1 = a_l(1, 0)$, $\mathbf{a}_2 = a_l(0.5, \sqrt{3})$, and $\mathbf{b}_1 = a_c(\cos\theta, \sin\theta)$, $\mathbf{b}_2 = a_c(\cos(\theta + \pi/3), \sin(\theta + \pi/3))$. The overall supercell-periodic structure can be realized if four integers exist which satisfy the matching condition $n_1\mathbf{a}_1 + n_2\mathbf{a}_2 = m_1\mathbf{b}_1 + m_2\mathbf{b}_2$. The ensuing supercell is

(n_1, n_2)	(m_1, m_2)	ρ	θ	N_p
(96,96)	(89,89)	0.92708333	0	7,921
(105,59)	(107,71)	0.92705245	2.54°	20,701
(96,72)	(100,54)	0.92705012	5.07°	18,316
(78,74)	(59,103)	0.92705113	9.78°	17,332

TABLE I. Parameters of the four supercells adopted for the simulations in PBC (see text for definitions). The supercells are determined following the procedure outlined in the text. For $\theta = 0$, the adopted mismatch $\rho = a_l/a_c = 89/96$ corresponds to the sixth approximation in the continued fraction expansion of $3/(1 + \sqrt{5})$.

that of a triangular lattice of size $L = |m_1\mathbf{b}_1 + m_2\mathbf{b}_2|$, containing a total number of particles $N_p = m_1^2 + m_1 m_2 + m_2^2$. In practice we fix $a_c = 1$ and vary $n_{1,2}$, $m_{1,2}$ in search of structures with a mismatch $\rho = a_l/a_c \approx 3/(1 + \sqrt{5})$ – close to the experimental values of Ref. 4 – and θ near the desired value, with the obvious additional constraint that the number of particles N_p should not be too large. We consider in practice the aligned configuration $\theta = 0$, plus the following misaligned configurations: $\theta \simeq 5°$, $\theta \simeq 10°$ and $\theta_{\text{opt}} \simeq 2.54°$. The latter is close to the (Novaco-McTague) equilibrium misalignment angle $\theta_{\text{NM}} \simeq 2.58°$ predicted by weak-coupling elastic theory.[18,19] Table I collects the adopted supercell parameters.

As mentioned earlier, the mismatch in this case produces a moiré pattern which could be roughly described as a patchwork or superlattice of small domains where colloids and corrugation are mutually (nearly) commensurate, separated by a network of anti-soliton lines whose thickness decreases with increasing corrugation strength. From the experimental point of view, the underdense regime chosen here for exemplification is better suited than the overdense case $\rho > 1$ where local compressions may lead to buckling of particles out of the plane, and where the energetics (not symmetrical with respect to $\rho > 1$) is less convenient. The initial step of our study is to identify the distorted colloid lattice configuration of lowest energy in presence of the corrugation. For that, we carry out $T = 0$ damped-dynamics simulations testing different protocols. In the first we increase the corrugation amplitude U_0 in steps $\Delta U = 0.018$ – eventually reduced near transition critical points – then reversing the sign of ΔU and decreasing U_0 back to zero in order to check for hysteresis across structural transitions. The maximum values of the corrugation considered is $U_{\text{max}} = 1$. In the second protocol we switch on abruptly the corrugation at given values of U_0 with the monolayer initially either undistorted or in a configuration previously fully relaxed at U_{max}. For each U_0 we eventually take the lowest-energy configuration. Eventually the best configurations were always obtained using the first protocol described above.
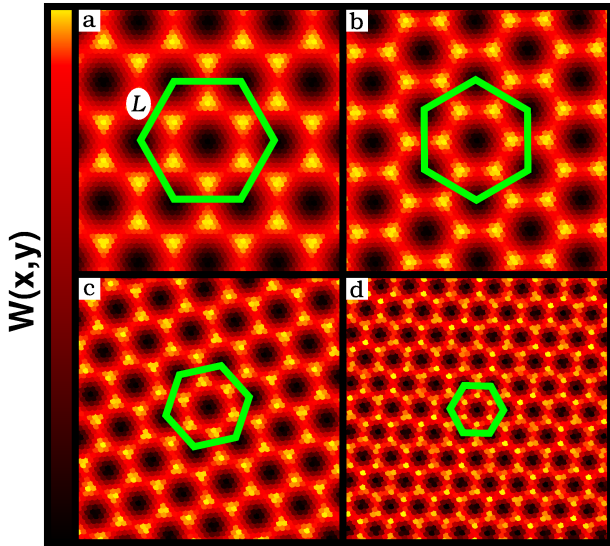
FIG. 2. (Color online) Examples of the moiré patterns obtained at $\rho \approx 0.927$ for misfit angles (a) $\theta = 0$, (b) $\theta_{\mathrm{opt}} \approx 2.54°$, (c) $\theta \approx 5°$, and (d) $\theta \approx 10°$. A small portion of the simulation supercells is displayed, containing an undistorted monolayer. The particles' colors reflect the underlying corrugation potential $W(x,y)$: dark for potential minima, bright for maxima. According to Eq. (1), at $\theta \simeq 2.54°$ the moiré orientation is $\psi \simeq 30°$. As θ increases the superstructure periodicity shrinks rapidly and rotates all the way to $\psi \simeq 60°$ (c).

The depinning of the monolayer is studied by applying to each colloid a driving force F_d, generally along a high-symmetry direction of the laser substrate potential. For a given value of U_0, the single particle barrier for the onset of motion is $F_{s1} = 8\pi U_0 / 9 a_l$. The external force is then increased adiabatically in steps $\Delta F = 0.002$, much lower than the lowest value of F_{s1} considered. The duration is fixed in such a way that a single free particle would slide by a total distance of $10\,a_c$. A colloid configuration is classified as sliding, when the procedure produces a final center-of-mass displacement $\Delta x_{\mathrm{cm}} \gtrsim 2\,a_c$.

Preliminary to presenting our results, it is useful to recall a few geometrical concepts. A given mismatch ρ and misalignment angle θ induce a specific moiré pattern of the colloidal crystal. The moiré superstructure of an undistorted monolayer is entirely described by its overall periodicity L and its orientation angle ψ relative to the substrate. Similar to the beats of two sinusoids in one dimension, the values of ψ and L are governed by the difference $\mathbf{G} - \mathbf{G}'$ between the smallest reciprocal lattice vectors of the monolayer and optical potential. The relations connecting ρ and θ to L and ψ are given for example in Ref. 24. Here we recall the angular relation

$$\cos\theta = \rho^{-1}\sin^2\psi + \cos\psi\sqrt{1 - \rho^{-2}\sin^2\psi}, \quad (1)$$

which, for $\rho \simeq 1$ produces a rapid reorientation of the moiré pattern for small changes of $\theta \simeq 0$, as visualized in
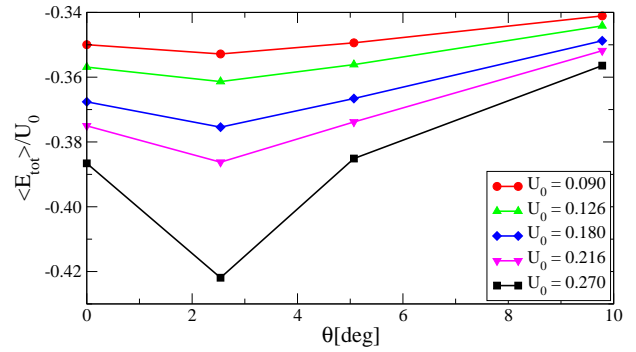

FIG. 3. (Color online) The total energy $\langle E_{\mathrm{tot}} \rangle$ per particle of the colloidal monolayer optimized in PBC, for a few misalignment angles θ. Curves correspond to increasing corrugation amplitude $U_0 \approx 0.1 - 0.3$. Energies are measured relative to that of the perfect crystal at $U_0 = 0$, and are scaled with respect to U_0 for better comparison.

Fig. 2.

III. RESULTS: THE TRANSITION IS STRUCTURAL

We begin by describing the evolution of the ground state configuration of our model underdense colloidal monolayer as a function of increasing corrugation strengths U_0, obtained at fixed incommensurability $\rho \simeq 0.927$ and for a grid of angular misalignment angles θ. Figure 3 shows the total potential energy per particle $\langle E_{\mathrm{tot}} \rangle$ as a function of U_0 and for several small θ values. The lowest energy is seen to occur at a small but finite θ_{opt}. This is a small but significant misalignment angle fairly close to the theoretical, weak-coupling misalignment θ_{NM} suggested by the theory of orientational epitaxy.[19–21] The detailed angular dependence of total colloid energy in the optical lattice was investigated in Ref. 18. The mainly longitudinal deformation for $\theta = 0$, is replaced in the optimal misalignment θ_{opt}, by energetically cheaper largely transverse deformations. This optimal misalignment angle is $\theta_{\mathrm{opt}} = 2.54°$, to a good approximation independent of corrugation U_0.

We wish to understand now what happens to the colloid structure, energy, and eventually to the static friction as a function of U_0 at $\theta = \theta_{\mathrm{opt}}$. For that purpose, we consider that the total potential energy per particle $\langle E_{\mathrm{tot}} \rangle = E_{\mathrm{tot}}/N_p$ is composed of two separate contributions:

$$\langle E_{\mathrm{tot}} \rangle = \langle W \rangle + \langle U_{\mathrm{pp}} \rangle, \quad (2)$$

where $\langle W \rangle$ is the average colloid-optical lattice interaction energy, and $\langle U_{pp} \rangle$ the average colloid-colloid repulsion. Figure 4a displays the two contributions to the total energy $\langle E_{\mathrm{tot}} \rangle$. The total energy evolution is smooth until $U_0 = 0.22$ where we observe a sudden decrease in
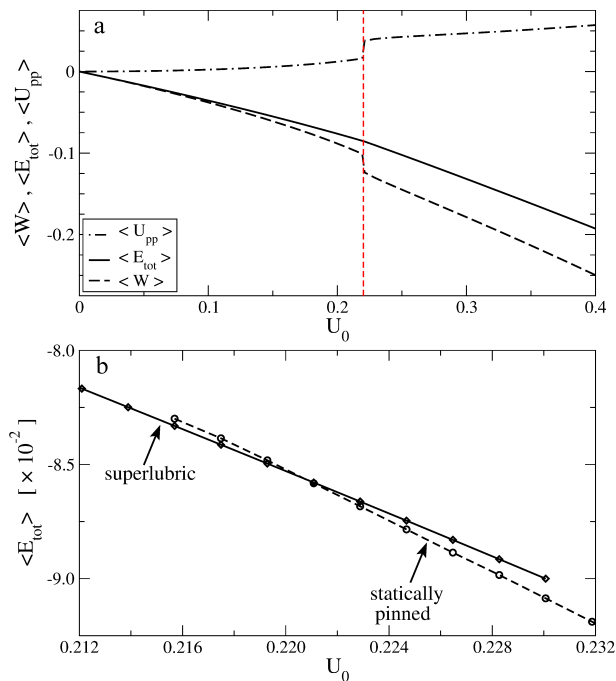
FIG. 4. (Color Online) (a) The total potential energy $\langle E_{\rm tot} \rangle$ per particle, its periodic-potential (corrugation) contribution $\langle W \rangle$, and interparticle contribution $\langle U_{\rm pp} \rangle$ as a function of the corrugation U_0 for the optimally misaligned colloidal monolayer ($\theta = \theta_{\rm opt} = 2.54°$). The sudden drop of $\langle W \rangle$ and the corresponding jump of $\langle U_{\rm pp} \rangle$ signal a first-order transition, taking place at constant incommensurability and misalignment angle. As will be shown later, the weak-corrugation phase is unpinned and superlubric, the strong-corrugation phase is pinned by a finite static friction. (b) The intersection between the total energy branches representing the superlubric (small U_0) and statically pinned (large U_0) structures. Like in all first-order transitions, each phase survives in metastable state beyond the transition point.

FIG. 5. (Color online) The moiré patterns of the fully-relaxed incommensurate colloid monolayer at $\theta_{\rm opt} = 2.54°$. A small portion of the simulation supercell is shown. Each dot represents a particle, colored according to the local corrugation potential $W(x,y)$: dark for potential minima, bright for maxima. (a) The optimal weak-corrugation configuration ($U_0 = 0.108$). (b) Zoomed-in region with arrows highlighting the particles' displacements (magnified 20×) from the ideal triangular lattice to the fully-relaxed configuration. Vortex-like displacements tend to locally rotate the domains back into registry with the substrate. (c) The optimal strong-corrugation state ($U_0 = 0.395$). The hexagonal domains appear now fully commensurate, and separated by sharp domain walls. Here most colloids fall very close to a potential minimum.

FIG. 6. (Color online) The average local orientation of the monolayer $\theta_{\rm loc}$ (see text for definition) plotted as a function of corrugation. The vertical dashed line separates the weak-corrugation and the strong-corrugation phases.

$\langle W \rangle$ accompanied by an increase of the repulsive term. This indicates a first-order structural transition in the monolayer. Figure 5a displays the $\theta_{\rm opt}$ moiré patterns of the relaxed monolayer for $U_0 = 0.108$, a weak corrugation well below the first-order transition. For this weak corrugation the triangular colloidal crystal is only slightly affected by the substrate potential. Panel 5b illustrates the corresponding colloid displacements relative to the rigid unperturbed crystal ($U_0 = 0$). The misalignment of the colloidal crystal over the lattice corrugation is only slightly modulated by a vortex-like distortion reflecting the shear nature of the solitons, whose width is larger than their separation. Panel 5c portrays the moiré pattern for $U_0 = 0.395$, a strong corrugation well above the transition. A hexagonal superlattice of domains of colloids locally commensurate with the corrugation are separated by "atomically" sharp antisolitons lines.
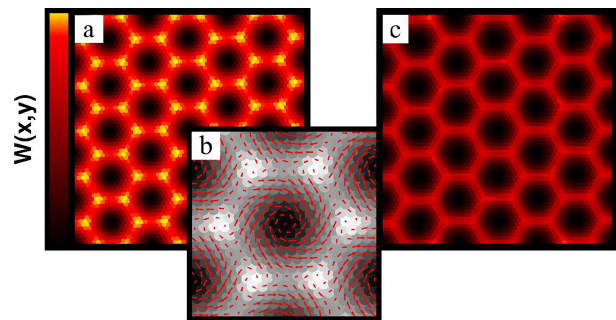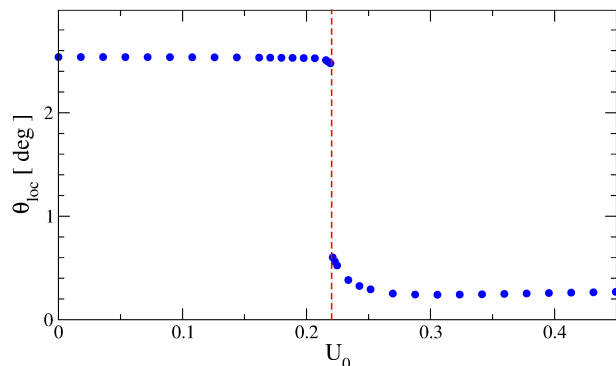
It is also instructive to look at the average local orientation of the monolayer (see Fig. 6), defined as

$$\theta_{\rm loc} = \frac{1}{M} \sum_{\langle i,j \rangle} {\rm mod}\left(\theta_{ij}, \frac{\pi}{3} \right), \qquad (3)$$

where the sum is over all M pairs $\langle i,j \rangle$ of nearest neighbor particles, and θ_{ij} is the angle between the relative position vector $\mathbf{r}_i - \mathbf{r}_j$ and the x-axis. At the transition, the commensurate domains realign significantly with the triangular potential. Figure 4b shows a crossing of the total energies of the weak-corrugation and the strong-corrugation phase at the transition point, as a function of
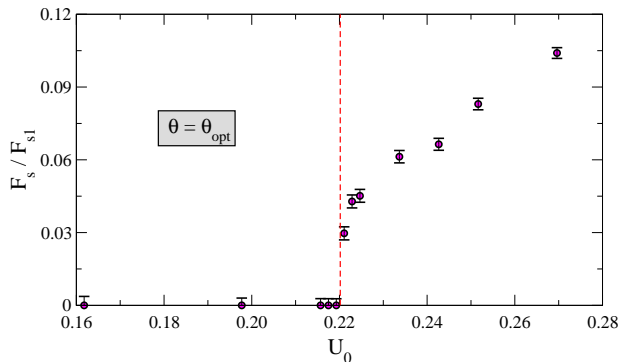
FIG. 7. (Color online) The static friction force F_s of the $\rho \simeq$ 0.927 colloidal monolayer, normalized to the single-particle barrier F_{s1}. The dashed line indicates the transition point corrugation $U_c = 0.22$ where the colloid monolayer suddenly locks onto the corrugation. The error bar is defined by the force increment $\Delta F = 0.002$ used in the simulation protocol.
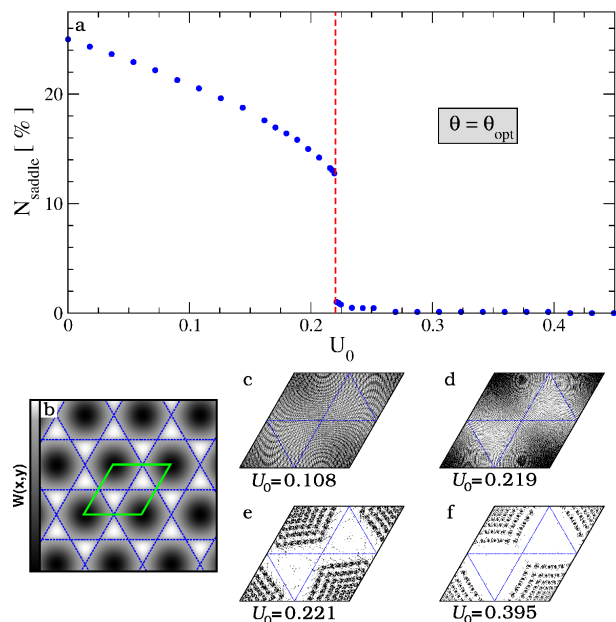

FIG. 8. (Color online) (a) The fraction of colloidal particles which sample repulsive regions of the substrate potential, i.e. those positions where $W(x,y)$ exceeds the saddle energy, plotted as a function of the corrugation strength U_0. (b) The triangular potential $W(x,y)$. Dark and bright regions correspond respectively to minima and maxima, isolines are reported at the saddle-point value and a primitive cell is highlighted at the center of the density plot. (c-f) The positions of the particles reported inside one primitive cell of the substrate potential. Configurations are shown for different corrugation values: (c) $U_0 = 0.108$ – superlubric phase; (d) $U_0 = 0.219$ – just below the transition; (e) $U_0 = 0.221$ – just above the transition; (f) $U_0 = 0.395$ – well above the transition.
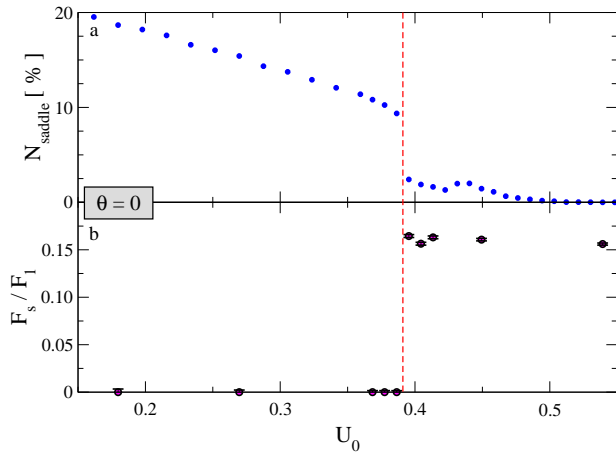
U_0. A separate stability analysis shows that each phase survives as a metastable state over a finite corrugation interval on the "wrong" side of U_c, eventually collapsing at its respective spinodal point.

IV.   RESULTS: SUPERLUBRICITY AND STATIC FRICTION

We now come to the static friction force F_s of the colloid monolayer, the main interest of the present investigation. It is obvious that the first-order structural transition uncovered in the previous section must affect it. Figure 7 shows the static friction force F_s obtained by simulation with $\rho \simeq 0.927$ and $\theta_{opt} = 2.54°$ as a function of the corrugation strength U_0. For weak corrugation $U_0 < U_c$ the static friction is small below the error. In this regime the colloid monolayer slides freely already at the smallest applied force, demonstrating that the incommensurate state is indeed superlubric.[25] At the transition corrugation the static friction suddenly jumps to $0.03F_{s1}$. The monolayer becomes pinned, and the superlubricity is lost through a first-order transition. Unlike 1D, where the pinning transition was of second order, here it coincides with the first-order structural transition.

Leaving the transition order aside, it is easy to show that the underlying reason for pinning in the present 2D case is still quite similar to that in the 1D FK model, namely a collapse of the dynamically-available phase space. In 1D, that collapse was signaled by the simultaneous collapse of the probability for any particle to occupy a local potential maximum. In the present 2D case we can similarly investigate the probability for colloids to occupy, in their optimal configuration, the (x,y) triangular region above the saddle-point among adjacent local minima of the corrugation potential. If the analogy with 1D holds, a superlubric, ergodic state should populate abun-

dantly this region, while in a pinned, broken-ergodicity state, the population probabilty at the center of these regions should collapse to zero, and even remain zero across a whole neighborhood of the maximum – a finite "disorder parameter".[8] Indeed, as shown in Fig. 8a, at the first-order superlubric-pinned transition, these repulsive regions around the maxima depopulate dramatically. This is represented pictorially in Fig. 8c-f, reporting the particles' positions folded in one primitive cell of the corrugation lattice (see Fig. 8b). These properties represent a 2D version of the disorder parameter Ψ, which measures the width of the largest gap appearing in the Hull function at the Aubry transition in the incommensurate 1D FK model.[8] It should be noted that in the pinned colloid state the static friction force remains well below the single-colloid limit value F_{s1}, as shown in Fig. 7. The reason for this lower static friction is that of course the monolayer sliding is still strongly collective, whereby the particles surrounding a given particle attempting to cross a forbidden region actually help by pushing it across the barrier.

FIG. 9. (Color online) Unrotated $\theta = 0$ mismatched colloid monolayer, $\rho \approx 0.927$. (a) Fraction of colloidal particles which populate repulsive regions of the corrugation potential (where $W(x,y)$ exceeds the saddle-point energy) plotted as a function of the corrugation strength U_0 across the superlubric-pinned transition. The dashed line marks the transition point $\tilde{U}_c = 0.391$. (b) Static friction force F_s, normalized to the depinning force F_{s1} of a single particle in the same periodic potential. Above the transition the monolayer locks onto the corrugation. The error bar is defined by the force increment $\Delta F = 0.001$ used in the simulation protocol.

V. RESULTS: STATIC FRICTION AT DIFFERENT MISALIGNMENTS

An interesting aspect of the transition to the 2D locked state is its dependence on the misfit angle θ. As discussed in Sect. III, at the optimal orientation θ_{opt} the colloidal crystal deforms mainly via the softer transverse modes, facilitating the interdigitation with the substrate. If the monolayer is rotated away from θ_{opt} its grip of the corrugation weakens: as a result the superlubric state survives up to a larger corrugation strength U_0. As the simplest example, consider the aligned monolayer configurations obtained at $\theta = 0$.

Figure 9a shows the evolution of the number of particles sampling repulsive regions of the corrugation potential. In this case too we identify a corrugation $\tilde{U}_c = 0.391$ above which the monolayer pins, again with a first-order transition. As expected, the transition corrugation is larger – almost a factor of two – than that at the optimal misalignment, $U_c = 0.22$. Figure 9b shows the static friction force F_s across the structural transition. The aligned monolayer is superlubric up to $\tilde{U}_c$, where we observe a sudden surge of the static friction F_s. Actually in this metastable aligned case the subsequent evolution of static friction becomes somewhat erratic. This behaviour can be explained as follows. A proliferation of energetically close metastable configurations – each characterized by its own static friction – is expected[9] above the transition point. While at θ_{opt} all protocols produced configurations with regularly-spaced hexagonal domains,
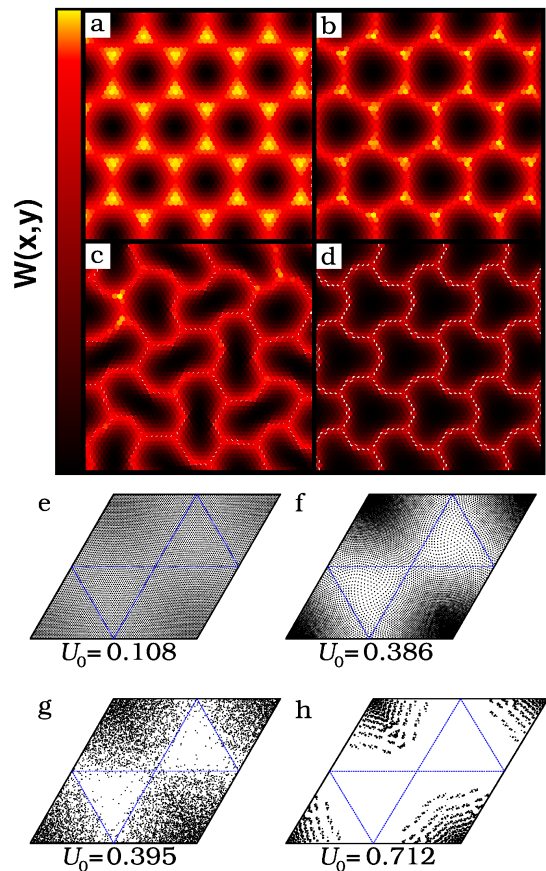

FIG. 10. (Color online) Panels (a-d): the moiré patterns of the fully relaxed monolayer at $\theta = 0$. A small portion of the simulation supercell is shown. Each dot represents a particle, colored according to the local corrugation potential $W(x,y)$: dark for potential minima, bright for maxima. Panels (e-h): the particles' positions are reported into one primitive cell of the substrate triangular potential. Configurations are shown for the following values of the corrugation: (a,e) $U_0 = 0.108$ – superlubric phase. (b,f) $U_0 = 0.386$ – just below the transition. (c,g) $U_0 = 0.395$ – just above the transition, where the energetically favored configuration consists of an arrangement of irregular domains. (d-h) $U_0 = 0.712$ – a strong-corrugation phase corresponding to an arrangement of regularly-shaped registered domains.

at $\theta = 0$ we observe several both irregular and regular arrangements of registered domains, which then happen to be energetically favored at different corrugation values U_0 (see Fig. 10c,d). Some fluctuations in F_s are therefore expected when one also considers that in incommensurate systems with many degrees of freedom, states with lower energy do not necessarily display a higher static friction force.[26] This complexity disappears below U_c where there always is a unique structure, shown in Fig. 10a,b, respectively away and close to the transition. Summing up this part, the evolution of the monolayer structure as a function of U_0 is highly sensitive to the misalignment angle.

VI. DISCUSSION AND CONCLUSIONS

Colloids in optical lattices are systems recently introduced, potentially representing powerful tools which may contribute to our understanding of friction between crystalline surfaces.[4,6,7,27] Colloidal monolayers in an incommensurate lattice corrugation potential are shown to represent ideal systems to study the superlubric-pinned transition, expected as a function of increasing corrugation strength, but never realized so far in any 2D system, under constant geometrical conditions. In 1D it is well known that at this transition the onset of a disorder parameter – measuring a region of phase space inaccessible to particle positions – impedes the dynamics of free-sliding motion, giving rise to static friction through a continuous phase transition.[8,9] In the 2D case of colloids we predict a transition of similar character, the main difference being now its first-order character. The relative alignment and misalignment of the two lattices plays an additional role. We found vanishingly small static friction up to a critical value U_c corresponding to a joint structural and dynamical transition of the monolayer. At the transition the colloidal crystal adapts to the periodic potential by a local rotation (back to registry) of the nearly commensurate domains forming the moiré of the incommensurate phase.

Similarly to the 1D case, pinning of the monolayer is due to a collapse to zero of the number of particles sampling the most repulsive regions of the periodic potential. These poorly placed particles are those which are easily set into motion in the superlubric phase. Their disappearance is therefore responsible for the arisal of static friction in the pinned state. Experimentally, vanishingly small values of F_s have been observed in 2D incommensurate structures,[7,11] but the realization and the analysis of the transition between superlubric and pinned states is missing to our knowledge. The present work suggests the possibility to pursue and investigate in detail the superlubric-pinned transition by gradually increasing the optical-lattice strength. Additional phenomena may be accessed by forcing rotations and modifying the natural misalignment of the colloidal crystal with respect to the optical lattice. Since the superlubric phase at $\theta \neq \theta_{\mathrm{opt}}$ survives up to larger corrugation values, rotations of mismatched sliders initially away from the optimal orientation might in fact end up in reentrant pinning as soon as θ_{opt} is hit, in a way similar to the matched case ($\rho = 1$, $\theta_{\mathrm{opt}} = 0$) of a rotated graphene flake sliding over graphite.[28]

[1] B. N. J. Persson, *Sliding Friction* (Springer, Berlin, 1998).

[2] A. Vanossi, N. Manini, M. Urbakh, S. Zapperi, and E. Tosatti, Rev. Mod. Phys. **85**, 529 (2013).

[3] M. Urbakh, and E. Meyer, Nat. Mat. **10**, 8 (2010).

[4] T. Bohlein, J. Mikhael, and C. Bechinger, Nat. Mat. **11**, 126 (2012).

[5] M. Reguzzoni, M. Ferrario, S. Zapperi, and M. C. Righi, Proc. Natl. Acad. Sci. USA **107**, 1311 (2010).

[6] J. Hasnain, S. Jungblut, and C. Dellago, Soft Matter **9**, 5867 (2013).

[7] A. Vanossi, N. Manini, and E. Tosatti, Proc. Natl. Acad. Sci. USA **109**, 16429 (2012).

[8] O. M. Braun and Y. Kivshar, *The Frenkel-Kontorova Model: Concepts, Methods, and Applications* (Springer, Berlin, 1998).

[9] S. Aubry and P. Y. Le Daeron, Physica D **8**, 381 (1983).

[10] K. Shinjo and M. Hirano, Surf. Sci. **283**, 473 (1993).

[11] M. Dienwiebel, G. S. Verhoeven, N. Pradeep, J. W. M. Frenken, J.A. Heimberg, and H.W. Zandbergen, Phys. Rev. Lett. **92**, 126101 (2004).

[12] R. Zhang, Z. Ning, Y. Zhang, Q. Zheng, Q. Chen, H. Xie, Q. Zhang, W. Qian, F. Wei, Nature Nanotech. **8**, 912 (2013).

[13] A. Nigues, A. Siria, P. Vincent, P. Poncharal, L. Bocquet, Nat. Mat. **13**, 688 (2014).

[14] D. Dietzel, C. Ritter, T. Mönninghoff, H. Fuchs, A. Schirmeisen, U. D. Schwarz, Phys. Rev. Lett. **101**, 125505 (2008).

[15] D. Dietzel, M. Feldmann, U. D. Schwarz, H. Fuchs, A. Schirmeisen, Phys. Rev. Lett. **111**, 235502 (2013).

[16] B. N. J. Persson, E. Tosatti, D. Fuhrmann, G. Witte, Ch. Wöll, Phys. Rev. B **59**, 11777 (1999).

[17] M. Pierno, L. Bruschi, G. Mistura, G. Paolicelli, A. di Bona, S. Valeri, R. Guerra, A. Vanossi, and E. Tosatti, Nat. Nanotech. **106**, 1 (2015).

[18] D. Mandelli, A. Vanossi, N. Manini, and E. Tosatti, Phys. Rev. Lett. **114**, 108302 (2015).

[19] A. D. Novaco and J. P. Mc Tague, Phys. Rev. Lett. **38**, 1286 (1977).

[20] H. Shiba, J. Phys. Soc. Jpn. **46**, 1852 (1979).

[21] H. Shiba, J. Phys. Soc. Jpn. **48**, 211 (1980).

[22] A. Vigentini, B. Van Hattem, E. Diato, P. Ponzellini, T. Meledina, A. Vanossi, G. Santoro, E. Tosatti, and N. Manini, Phys. Rev. B **89**, 094301 (2014).

[23] G. Trambly de Laissardière, D. Mayou, and L. Magaud, Nano Lett. **10**, 804 (2010).

[24] F. Grey and J. Bohr, Europhys. Lett. **18**, 717 (1992).

[25] Strictly speaking, since we are adopting PBC, our systems are commensurate and therefore ultimately pinned. A fine search at $U_0 = 0.216$, below and close to U_c, shows that the static friction force is indeed finite there, being $0.0005 < F_s < 0.001$. However, this "pinning transition" is marked by a sudden increase in F_s by two-three orders of magnitude when increasing U_0 above the critical value U_c.

On the opposite side, for $U_0 \ll U_c$, F_s is so small that it is quite hard to measure.

[26] O. Braun, M. Paliy, and B. Hu, Phys. Rev. Lett. **83**, 5206 (1999).

[27] J. Hasnain, S. Jungblut, A. Tröster, and C. Dellago, Nanoscale **6**, 10161 (2014).

[28] A. E. Filippov, M. Dienwiebel, J. W. M. Frenken, J. Klafter, and M. Urbakh, Phys. Rev. Lett. **100**, 046102 (2008).